

Dual Regulation of Actin Rearrangement through Lysophosphatidic Acid Receptor in Neuroblast Cell Lines: Actin Depolymerization by Ca^{2+} - α -Actinin and Polymerization by Rho

Nobuyuki Fukushima,^{*†} Isao Ishii,^{†§} Yoshiaki Habara,^{||} Cara B. Allen,[¶] and Jerold Chun^{†¶#@}

^{*}Department of Molecular Biochemistry, Hokkaido University Graduate School of Medicine, Sapporo 060-8638, Japan; [†]Department of Pharmacology, [¶]Neurosciences Program, [#]Biomedical Sciences Program, School of Medicine, University of California, San Diego, La Jolla, California 92093-0636; [@]Molecular Neuroscience, Merck Research Laboratories, San Diego, California 91212; and ^{||}Department of Biomedical Sciences, Hokkaido University Graduate School of Veterinary Medicine, Sapporo 060-0818, Japan

Submitted September 24, 2001; Revised April 11, 2002; Accepted April 22, 2002
Monitoring Editor: Howard Riezman

Lysophosphatidic acid (LPA) is a potent lipid mediator with actions on many cell types. Morphological changes involving actin polymerization are mediated by at least two cognate G protein-coupled receptors, $\text{LPA}_1/\text{EDG-2}$ or $\text{LPA}_2/\text{EDG-4}$. Herein, we show that LPA can also induce actin depolymerization preceding actin polymerization within single TR mouse immortalized neuroblasts. Actin depolymerization resulted in immediate loss of membrane ruffling, whereas actin polymerization resulted in process retraction. Each pathway was found to be independent: depolymerization mediated by intracellular calcium mobilization, and α -actinin activity and polymerization mediated by the activation of the small Rho GTPase. α -Actinin-mediated depolymerization seems to be involved in growth cone collapse of primary neurons, indicating a physiological significance of LPA-induced actin depolymerization. Further evidence for dual regulation of actin rearrangement was found by heterologous retroviral transduction of either *lpa*₁ or *lpa*₂ in B103 cells that neither express LPA receptors nor respond to LPA, to confer both forms of LPA-induced actin rearrangements. These results suggest that diverging intracellular signals from a single type of LPA receptor could regulate actin depolymerization, as well as polymerization, within a single cell. This dual actin rearrangement may play a novel, important role in regulation of the neuronal morphology and motility during brain development.

INTRODUCTION

Lysophosphatidic acid (LPA), a simple yet potent bioactive phospholipid, has been shown to elicit diverse cellular re-

sponses in many types of cells (Moolenaar, 1995; Moolenaar *et al.*, 1997; Contos and Chun, 1998; Moolenaar, 1999). These responses are mediated by specific cell-surface G protein-coupled receptors, which are encoded by three cognate genes: *lpa*₁/*edg-2*, *lpa*₂/*edg-4*, and *lpa*₃/*edg-7* (Hecht *et al.*, 1996; An *et al.*, 1998; Contos and Chun, 1998; Bandoh *et al.*, 1999; Chun, 1999; Chun *et al.*, 1999; Fukushima *et al.*, 2001). LPA_1 shares many downstream intracellular signaling pathways with LPA_2 , including inhibition of adenylyl cyclase (AC) and activation of phospholipase C (PLC) and the small GTPase Rho (Fukushima *et al.*, 1998, 2001; Ishii *et al.*, 2000). In contrast, LPA_3 links to the former two pathways: AC inhibition and PLC activation, but not Rho stimulation (Ishii *et al.*, 2000).

One prominent cellular response evoked by LPA is rearrangement of the actin cytoskeleton. In fibroblasts, LPA induces actin polymerization, resulting in the formation of

Article published online ahead of print. Mol. Biol. Cell 10.1091/mbc.01-09-0465. Article and publication date are at www.molbiol-cell.org/cgi/doi/10.1091/mbc.01-09-0465.

[†] Corresponding author. E-mail address: nfuku@med.hokudai.ac.jp.

[§] Present address: Department of Molecular Genetics, National Institute of Neuroscience, 4-1-1 Ogawahigashi, Kodaira, Tokyo 187-8502, Japan

Abbreviations used: BAP, bacterial alkaline phosphatase; CD, cytochalasin D; DIC, differential interference contrast; ECM, extracellular matrix; EGFP, enhanced green fluorescent protein; f-actin, filamentous actin; LPA, lysophosphatidic acid; PKC, protein kinase C; PLC, phospholipase C; PTX, pertussis toxin.

cytoplasmic stress fibers that consist of filamentous actin (f-actin) and are associated with cell contraction (Ridley and Hall, 1992). In neuroblastoma cells or primary neuroblasts, LPA induces actin polymerization that produces neurite retraction/cell rounding (Jalink *et al.*, 1993; Fukushima *et al.*, 1998, 2000). In both cell types, LPA induces actin polymerization through the activation of Rho and its downstream Rho-associated kinase (Amano *et al.*, 1997; Hirose *et al.*, 1998). One difference between these cell types is the amount of f-actin that is present under resting conditions. Unlike resting fibroblasts that have little f-actin, resting neuronal cells have abundant f-actin throughout their cell bodies, in both cytoplasm and processes (Jalink *et al.*, 1993; Fukushima *et al.*, 1998, 2000). This raises the question of how LPA affects preexisting abundant f-actin during the remodeling of neuronal cell morphology. In addition, the intracellular actions of LPA through direct interactions with actin-binding proteins have been demonstrated (Meerschaert *et al.*, 1998). Herein, we provide the first evidence that LPA induces both actin depolymerization and polymerization within a single neuronal cell through distinct, receptor-mediated signaling pathways. Actin depolymerization further seems to be involved in regulation of neuronal growth cone morphology.

MATERIALS AND METHODS

Cell Cultures

TR mouse cerebral cortical immortalized neuroblast cells and B103 rat neuroblastoma cells were grown as described previously (Chun and Jaenisch, 1996; Hecht *et al.*, 1996; Fukushima *et al.*, 1998; Ishii *et al.*, 2000). Cells were maintained in DMEM (Invitrogen, Carlsbad, CA) containing 10% fetal calf serum and penicillin/streptomycin. For experiments, cells were grown on (poly)lysine-coated glass coverslips (12 or 40 mm in diameter, 500 cells/coverslip, unless stated otherwise; Fisher Scientific, Tustin, CA). The next day, cells were washed with serum-free Opti-MEM I (Invitrogen) supplemented with 55 μ M β -mercaptoethanol, 20 mM glucose, and penicillin/streptomycin, and were further incubated in the serum-free medium for 1 d before analyses. Primary cortical neurons were prepared using embryonic day 12 mice as described previously (Fukushima *et al.*, 2000), seeded on Cell-TaK (BD Biosciences, Franklin Lakes, NJ)-coated glass coverslips (12 mm in diameter, 500-2000 cells/coverslip), and cultured in Opti-MEM containing 5% fetal calf serum.

Time-Lapse Video Microscopy

Time-lapse, video-enhanced differential interference contrast (DIC) microscopy was carried out as described previously (Fukushima *et al.*, 2000). The 40-mm coverslips were mounted onto a heat-controlled perfusion apparatus (FCS-2; Bioprotechs, Butler, PA) set at 37°C, and cells were observed with an inverted microscope (Axiovert 135; Carl Zeiss, Thornwood, NY) by using a 63 \times oil immersion objective (Plan-Apochromat; Carl Zeiss). Replacement of culture medium with a buffer containing 0.1% fatty acid-free bovine serum albumin (Sigma-Aldrich, St. Louis, MO) was manually performed with a syringe (~2 ml/min). DIC images were collected every 15 s with a cooled charge-coupled device camera (DEI-47; Carl Zeiss) by using the Scion Image software (Scion, Frederick, MA).

Immunocytochemistry

Cells were fixed for 15 min with 3.7% formaldehyde in the presence of 0.5% Triton X-100 and were then washed with phosphate-buffered saline. To visualize f-actin, cells were incubated with Alexa Fluor 546-labeled phalloidin (1 U/ml; Molecular Probes, Eugene,

OR). For double-labeling studies, cells were blocked with 10% normal goat serum and 0.5% bovine serum albumin and incubated for 2 h with a primary antibody. The antibody used was an anti- α -actinin monoclonal antibody (mAb) (1:300; Sigma-Aldrich), anti-gelsolin mAb (2 μ g/ml; BD Biosciences), anti-GFP polyclonal antibody for labeling enhanced green fluorescent protein (EGFP) (1:1000; CLONTECH, Palo Alto, CA), or anti-FLAG M2 mAb (1 μ g/ml; Sigma-Aldrich). Cells were further incubated with biotinylated anti-mouse IgM, anti-rabbit IgG, or anti-mouse IgG antibodies (5 μ g/ml; all from Vector Laboratories, Burlingame, CA), followed by incubation with Alexa 488 streptavidin (1 μ g/ml; Molecular Probes) and Alexa 546 phalloidin. For double labeling of transfected TR cells for FLAG and α -actinin, cells were first labeled for FLAG. Cells were then incubated with anti- α -actinin antibody, followed by incubation with Cy3-labeled anti-mouse IgM antibody (1.5 μ g/ml; Jackson Immunoresearch Laboratories, West Grove, PA). For double labeling of B103 cells for EGFP and α -actinin, cells were first labeled for EGFP and then stained for α -actinin. Approximately 200 cells/coverslip were observed with an inverted microscope (Axiovert 135) and a 40 \times objective (Plan NEOFLUAR; Carl Zeiss), and counted in at least five fields, which were selected randomly, but substantially in the middle, top, and bottom of the middle and right and left of the middle of coverslips. Cells were also photographed using a 40 \times (Plan NEOFLUAR) or 63 \times oil immersion objective (Plan-Apochromat) and Cy3 or fluorescein filters, and jpg format images created. In some cases, fluorescent images were captured using a charge-coupled device camera (DXM1200; Nikon, Tokyo, Japan) and software ACT-1 (version 2.0; Nikon), and converted to jpg files. All figures of stained cells were generated by using Adobe Photoshop 6.0 (Adobe Systems, Mountain View, CA).

Ca²⁺ Imaging

Cells were cultured on 40-mm coverslips, loaded with 10–20 μ M fura 2-acetoxymethyl ester, and subjected to Ca²⁺ image analysis (Habara and Kanno, 1991). Briefly, the coverslip was mounted onto a heat-controlled perfusion apparatus (FCS-2; 35°C), and fluorescence images were analyzed by the digital image processor (Argus-100/Ca; Hamamatsu Photonics, Hamamatsu, Japan). The buffer was Opti-MEM I (without phenol red) containing 0.1% fatty acid-free bovine serum albumin. LPA stimulation was performed by the replacement with LPA (1 μ M)-containing buffer at 2 ml/min. The images were collected at a 30-s interval before (2 images) and after LPA exposure (12 images) and displayed using pseudocolor.

PLC Assay

TR cells on 12-well plates were prelabeled with [³H]inositol (2 μ Ci/well), stimulated with LPA for 20 min, and radioactivity in the inositol phosphate fractions measured, as described previously (Ishii *et al.*, 2000).

Rho Assay

Cells on 40-mm (poly)lysine-coated coverslips (20,000 cells seeded/coverslip) were stimulated with LPA and lysed in 500 μ l of Rho-binding buffer (50 mM Tris-HCl, 500 mM NaCl, 10 mM MgCl₂, 1% Triton X-100, 0.5% sodium deoxycholate, 0.1% SDS, and 1 \times protease inhibitor cocktail, pH 7.2). Cell lysates were centrifuged and the resultant supernatants (450 μ l) incubated with agarose beads-conjugated rhotekin Rho binding domain (Upstate Biotechnology, Lake Placid, NY) for 45 min on ice. The beads were washed four times and bead-bound, GTP-bound active forms of Rho specifically detected by Western blot analysis by using anti-RhoA mAb (50 ng/ml; Santa Cruz Biotechnology, Santa Cruz, CA), peroxidase-labeled anti-mouse IgG antibody (100 ng/ml; Vector Laboratories), and ECL Plus (Amersham Biosciences, Piscataway, NJ), according the manufacturers' protocols. An aliquot (15 μ l) of the cell lysates was used for detection of total amounts of Rho.

Construction of FLAG-tagged α -Actinin Expression Plasmids

Chick nonmuscle α -actinin cDNA (Waites *et al.*, 1992) was a kind gift from Dr. David R. Critchley (University of Leicester, Leicester, United Kingdom). A full-length α -actinin DNA that encodes 893 amino acids and an α -actinin mutant DNA that lacks Ca^{2+} -binding domain sequences and encodes 711 amino acids [designated herein as α -actinin^(-EP)] were amplified with polymerase chain reaction by using Platinum *Taq* DNA polymerase high-fidelity (Invitrogen). They were subcloned in frame into the *NotI/XbaI* and *NotI/Clal* sites of a pFLAG-CMV-2 mammalian expression vector (Sigma-Aldrich), respectively. The nucleotide sequences were confirmed by BigDye terminator cycle sequencing (Applied Biosystems, Foster City, CA).

Transfection of TR Cells or Primary Cortical Neurons

TR cells were transfected with expression plasmids by using LipofectAMINE PLUS (Invitrogen). Cells were seeded on (poly)lysine-coated glass coverslips (500 cells/12 mm in diameter for immunostaining or 20,000 cells/40 mm in diameter for Western blotting) and incubated for 15 h with DNA-lipid complex (0.1 μg of DNA-1 μl of PLUS reagent-0.5 μl of LipofectAMINE/cm²). Cells were washed and further cultured in serum-free medium for 1 d before use. Transfection of cortical neurons was performed 3 d after seeding using LipofectAMINE2000 (0.15 μg of DNA-0.4 μl of lipid/cm²; Invitrogen). Cells were washed after 24 h and further cultured in serum-free Opti-MEM for 1 d before use.

f-Actin Binding Assay

TR cells on a 9-cm dish were transfected with expression plasmids by using LipofectAMINE2000. Cells were sonicated in 100 μl of lysis buffer (50 mM Tris-Cl, 0.6 M KCl, 1 mM EDTA, 1% Triton X-100, 0.5% deoxycholate-Na, and 1 \times protease inhibitor cocktail, pH 7.4), and cell lysates diluted with 500 μl of lysis buffer without KCl and deoxycholate-Na. FLAG-tagged proteins were immunoprecipitated using anti-FLAG M2 antibody (3 μg) and protein G-agarose (Santa Cruz Biotechnology) and eluted in 0.1 M glycine-HCl containing 0.1% Triton X-100, pH 3.5. The elutes (100 μl) were neutralized with 10 μl of 0.6 M Tris-Cl, pH 8.2, and subjected to f-actin binding assay. Eluted proteins (40 μl) were incubated with f-actin (10 μg) in 200 μl of binding buffer (20 mM Tris-Cl, 2 mM MgCl₂, 1 mM EDTA, and 0.5 mM dithiothreitol, pH 7.4) with or without 1.1 mM CaCl₂ for 1 h on ice. f-Actin was prepared by incubating rabbit muscle actin (Sigma-Aldrich) in polymerization buffer (5 mM Tris-Cl, 1 mM MgCl₂, 50 mM KCl, and 1 mM ATP, pH 8) at 4°C for 4 h. Reaction mixtures were centrifuged at 65,000 rpm (TLA 100.3; Beckman Coulter, Fullerton, CA) for 1 h and the supernatants (unbound proteins) precipitated by adding trichloroacetic acid. The trichloroacetic acid precipitates and ultracentrifuge precipitates (f-actin-bound proteins) were analyzed by Western blot analysis by using anti-FLAG M2 antibody (50 ng/ml). Bound antibodies were visualized by subsequent incubation with peroxidase-labeled anti-mouse IgG antibody and ECL plus. Images were captured by using ATTO Light Capture (AE-6960; ATTO, Tokyo, Japan).

Western Blotting

Cells were harvested in phosphate-buffered saline and mixed with 2 \times SDS-sample buffer (Laemmli, 1970). Cell extracts (50 μg of protein) were separated on 10% polyacrylamide gels, and proteins were transferred to polyvinylidene difluoride membranes (Millipore, San Jose, CA), which was followed by probing with anti-FLAG M2 antibody. Membranes were further incubated with peroxidase-labeled anti-mouse IgG antibody and ECL plus and exposed to x-ray films.

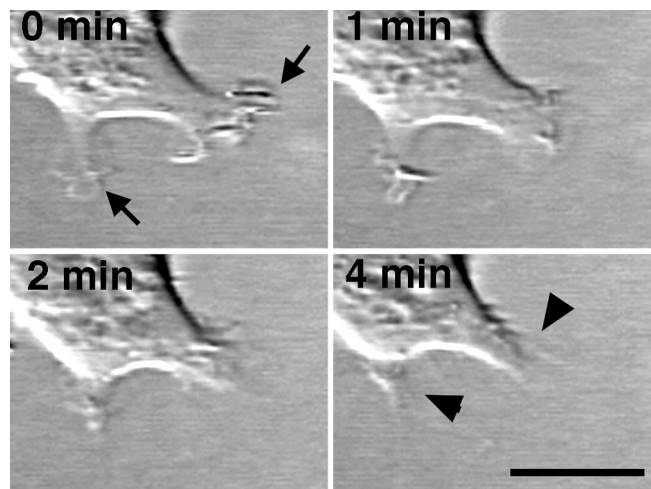


Figure 1. LPA induces a rapid loss of membrane ruffling in TR cells. Cells were treated with 0.5 μM LPA and cell morphology monitored by DIC microscopy. Arrows indicate membrane ruffling. Arrowheads indicate retracted processes that have lost membrane ruffling. Bar, 10 μm .

Infection of B103 Cells with Retroviruses Expressing LPA Receptors

Production of retroviruses expressing LPA₁ or LPA₂ and infection of B103 cells with these viruses were performed as described previously (Ishii *et al.*, 2000).

Reagents

LPA was purchased from Avanti Polar Lipids (Alabaster, AL). Cytochalasin D, pertussis toxin, bisindolylmaleimide I (Go6850), 1,2-bis(2-aminophenoxy)ethane-*N,N,N',N'*-tetraacetic acid-acetoxymethyl ester (BAPTA-AM), R-(+)-trans-N-(4-pyridyl)-4-(1-aminoethyl)-cyclohexane carboxamide (Y27632), and genistein were purchased from Calbiochem (La Jolla, CA).

RESULTS

Effects of LPA on Cell Shape and Actin Cytoskeleton

To examine the effects of LPA on neuronal cell morphology, we used TR cells, which are immortalized neuroblasts derived from embryonic mouse cerebral cortex (Chun and Jaenisch, 1996; Hecht *et al.*, 1996; Ishii *et al.*, 2000). TR cells extend their bipolar or multipolar processes on (poly)lysine-coated glass coverslips under serum-free culture condition (Chun and Jaenisch, 1996; Ishii *et al.*, 2000). These cells express *lpa*₁ and *lpa*₂ but not *lpa*₃, and respond to LPA with rapid retraction of their processes, resulting in cell rounding (Hecht *et al.*, 1996; Ishii *et al.*, 2000). Closer observation of TR cells revealed that most cells possess membrane ruffling at the tips of processes (Figure 1). After LPA exposure, these structures began to disappear within 1 min and completely disappeared by 4 min (Figure 1). In contrast, the well-documented phenomenon of process retraction (Hecht *et al.*, 1996; Ishii *et al.*, 2000) was also detectable at 1 min after LPA stimulation and was completed by 10–15 min, resulting in cell rounding (see below). LPA-induced loss of membrane

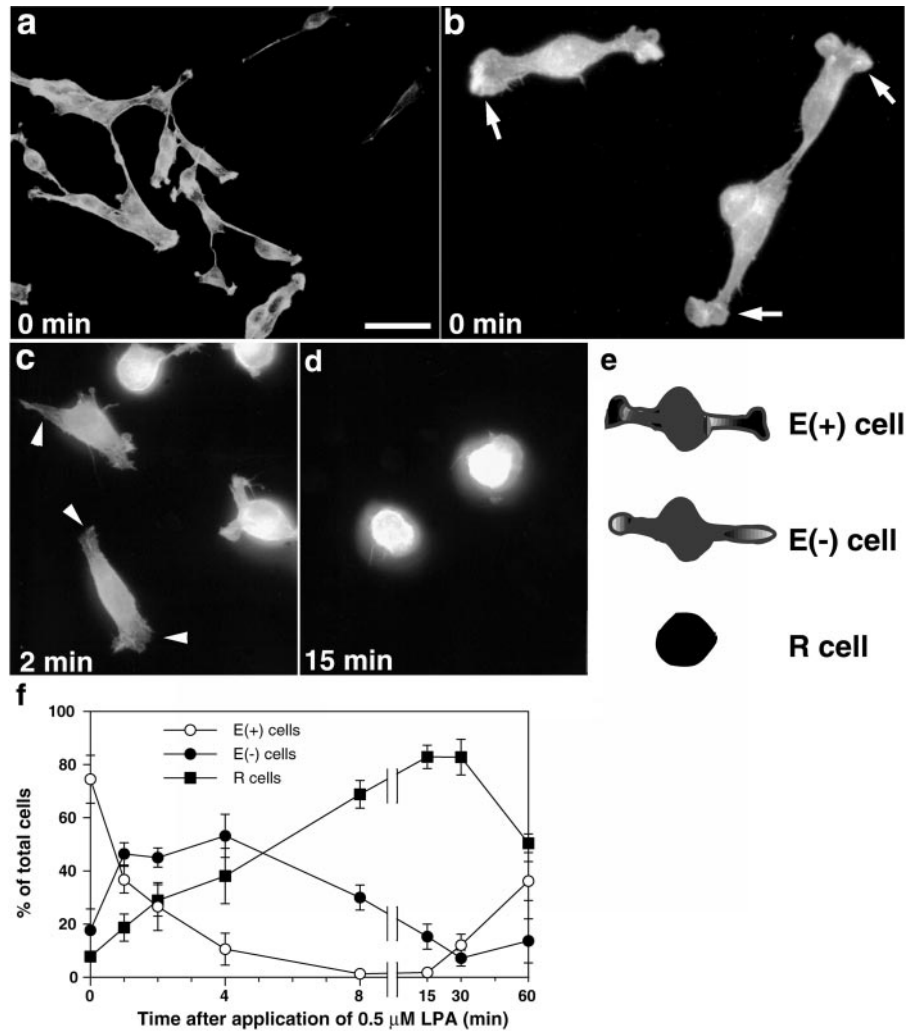


Figure 2. LPA induces actin rearrangement in TR cells. (a–d) f-Actin labeling of cells treated without (a and b) or with 0.5 μ M LPA for 2 min (c) or 15 min (d). Arrows (b) indicate f-actin-enriched membrane ruffling. Arrowheads (c) indicate processes without enriched f-actin. (e) Classification of three typical cell shapes: E(+) cells, cells with extended processes with f-actin-enriched membrane ruffling; E(-) cells, cells with extended processes without f-actin-enriched membrane; and R cells, cells with rounded cell bodies without processes. Graded shading shows accumulation of f-actin. (f) Time course of LPA-induced changes in populations of E(+), E(-), and R cells. Data are the means \pm SEM (n = 8). Bar, 50 μ m (a) and 20 μ m (b–d).

ruffling was also observed in TSM cells (Chun and Jaenisch, 1996), another immortalized neuroblast cell type derived from cerebral cortex (our unpublished data). Because membrane ruffling has been shown to contain enriched actin microfilaments (Bray, 1992; Matsudaira, 1994), we examined actin rearrangement during the loss of membrane ruffling.

TR cells were labeled with Alexa Fluor 546 phalloidin, allowing the visualization of f-actin (Figure 2). In most of the resting (control) cells, f-actin was distributed throughout cell bodies and was particularly enriched within membrane ruffling (Figure 2, a and b). This type of labeling was observed in \sim 75% of total cells, with the remaining cells showing no prominent staining at the tips (\sim 15%) or rounded morphologies without processes (\sim 10%). In this study, cells with these three typical morphologies are referred to as E(+) (extended process with f-actin-enriched membrane ruffling), E(-) (extended processes without f-actin-enriched membrane ruffling), and R (rounded cell body) (Figure 2e).

One to four minutes after 0.5 μ M LPA exposure, E(+) cell population decreased, whereas E(-) cell population increased (Figure 2, c and f). The f-actin staining observed in E(-) cells was indistinguishable from that observed in cells treated with 200 nM

cytochalasin D (CD) (our unpublished data), a drug that promotes actin depolymerization and also inhibits actin polymerization. This suggested that LPA rapidly induced actin depolymerization within ruffling membranes, as CD did (Figure 3a). The E(+) cell population decreased between 4 and 15 min and then increased, whereas the E(-) cell population decreased to a basal level between 4 and 60 min (Figure 2f). In contrast, the R cell population reached a peak at 15–30 min and then gradually decreased (Figure 2, d and f). The increase in the R cell population at 15 min was significantly inhibited by pretreatment with CD (Figure 3c), consistent with previous results showing that process retraction and cell rounding require actin polymerization (Jalink et al., 1994). These results indicated that LPA induced rapid actin depolymerization that was associated with loss of membrane ruffling, which was followed by actin polymerization that induced process retraction and cell rounding.

Effects of BAPTA-AM and Y27632 on LPA-induced Actin Cytoskeletal Changes

LPA receptors drive multiple signaling pathways through several types of G proteins, including $G_{i/o}$, G_{q} , and $G_{12/13}$

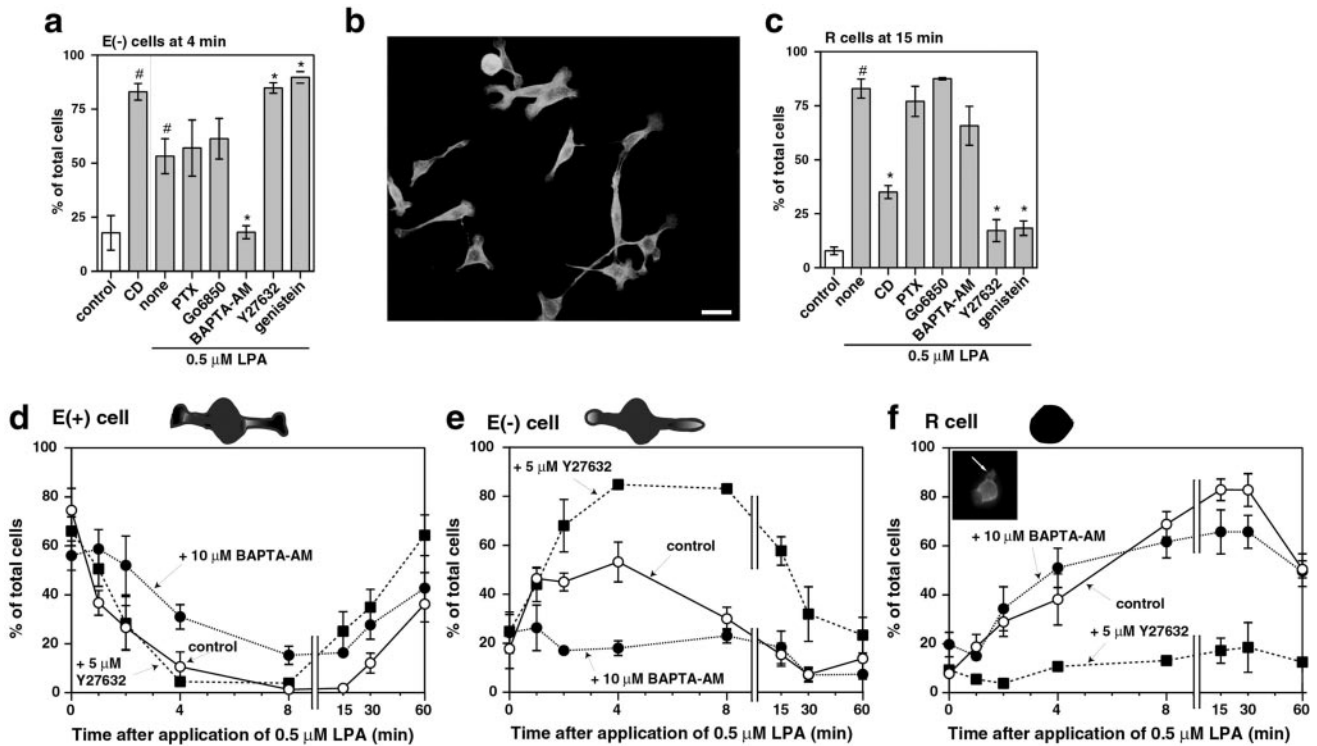


Figure 3. BAPTA-AM inhibits a loss of membrane ruffling, whereas Y27632 inhibits process retraction in LPA-stimulated TR cells. (a) Effects of various specific inhibitors on E(-) population. To examine effects of CD alone, cells were treated with 200 nM CD for 4 min. After pretreatment with inhibitors (100 ng/ml PTX for 18 h, 100 nM Go6850 for 5 min, 10 μ M BAPTA-AM for 5 min, 5 μ M Y27632 for 5 min, and 100 μ M genistein for 5 min), cells were stimulated with 0.5 μ M LPA for 4 min. Fixed cells were labeled for f-actin, and E(-) cells were counted at 4 min. Data are the means \pm SEM (n = 3–6). #p < 0.05 vs. control (no treatment) and *p < 0.05 vs. none (LPA alone). (b) f-Actin labeling of Y27632-pretreated cells exposed to LPA for 4 min. (c) Effects of various specific inhibitors on R population. Cells were pretreated with inhibitors, as described in the legend of a. CD was pretreated for 5 min. Cells were stimulated with 0.5 μ M LPA for 15 min and R cells counted. Data are the means \pm SEM (n = 3–6). #p < 0.05 vs. control (no treatment) and *p < 0.05 vs. none (LPA alone). (d–f) Time course of LPA-induced changes in populations of E(+), E(-), and R cells when pretreated with BAPTA-AM or Y27632. Fixed cells were labeled for f-actin, and E(+), E(-), and R cells were counted (d, e, and f, respectively). Data are the means \pm SEM (n = 4–8). (f, inset) Typical cell type that has a retracted process but still retains a small portion of f-actin-enriched membranes indicated by an arrow. This population likely resulted from retraction of processes with f-actin-enriched structures and was categorized as R cells. Bar, 25 μ m.

(Contos *et al.*, 2000; Ishii *et al.*, 2000; Fukushima *et al.*, 2001). The $G_{i/o}$ pathway is predominantly linked to mitogen-activated protein kinase activation and AC inhibition, but not to actin rearrangement (Weiner and Chun, 1999; Ishii *et al.*, 2000). The G_q pathway is linked to PLC activation (Ishii *et al.*, 2000; Kimura *et al.*, 2001), which leads to intracellular Ca^{2+} mobilization and protein kinase C (PKC) activation. These molecules can modulate actin rearrangement by means of Ca^{2+} -sensitive, actin-associated proteins such as α -actinin or gelsolin, and by phosphorylation of these proteins (Janmey, 1994; Keenan and Kelleher, 1998). The $G_{12/13}$ pathway activates Rho and Rho-associated kinases (ROCKs), resulting in actin polymerization (Gohla *et al.*, 1998; Kranenburg *et al.*, 1999). Specific pharmacological inhibitors, which are well established and widely used, were used to determine which pathways were involved in LPA-induced actin depolymerization.

Pretreatment of cells with pertussis toxin (PTX), which inhibits $G_{i/o}$ activation (Katada *et al.*, 1986), did not alter LPA-induced changes in the E(-) or R cell populations (Figure 3, a and c). Pretreatment of cells with a PKC inhibitor

Go6850 (Toullec *et al.*, 1991) also failed to alter the changes in those populations (Figure 3, a and c). At the used concentration (100 nM), this compound shows high selectivity for PKC but does not affect other kinases (Toullec *et al.*, 1991). These results indicated that both $G_{i/o}$ and PKC pathways were not involved in LPA-induced actin rearrangement. In contrast, when cells were pretreated with BAPTA-AM, which is known to prevent LPA-induced increase in intracellular Ca^{2+} concentrations in many types of cells (Manning and Sontheimer, 1997; Shahrestanifar *et al.*, 1999), LPA-induced transient increases in the numbers of E(-) cells were completely blocked (Figure 3, a and e). The E(+) cell population remained at relatively higher percentages in BAPTA-AM-treated cells compared with the percentages found in control cells (Figure 3d). The R cell population increased with time in BAPTA-AM-treated cells, similar to that in control cells (Figure 3f). Treatment with BAPTA-AM alone did not significantly affect the populations of E(+), E(-), and R, suggesting that this compound showed no effect on actin rearrangement under the resting conditions. These results indicated that Ca^{2+} signaling was involved in

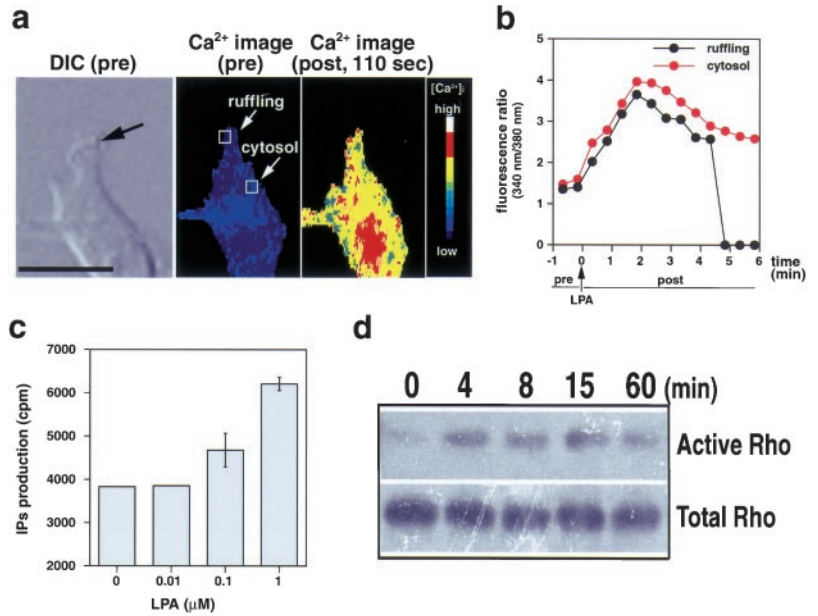


Figure 4. Increase in Ca²⁺ mobilization and Rho activity by LPA in TR cells. (a) Effects of LPA on Ca²⁺ mobilization. Cells were loaded with fura 2-acetoxymethyl ester and subjected to Ca²⁺ image analyses. DIC and Ca²⁺ images before LPA (1 μM) exposure and Ca²⁺ image 110 s after LPA exposure are shown. Note an increase in Ca²⁺ concentration within membrane ruffling after LPA exposure. An arrow indicates membrane ruffling. (b) Time course of fluorescence ratio. Fluorescence ratios (340 nm/380 nm) were determined within small portions in membrane ruffling and cytosol squared in a. The drop of ratio in the ruffling after 5 min is due to the disappearance of cell structures by process retraction. (c) Effects of LPA on PLC activity. Cells were labeled with [³H]inositol and stimulated with LPA, and PLC activity was measured as accumulation of radiolabeled total inositol phosphates (IPs). (d) Effects of LPA on Rho activity. Cells were stimulated with LPA for the indicated time and extracted for the detection of active and total Rho. Bar, 20 μm.

LPA-induced actin depolymerization but not actin polymerization. Consistent with this, thapsigargin, a reagent that depletes Ca²⁺ stores and increases intracellular Ca²⁺ concentrations (Thastrup et al., 1990), induced the loss of membrane ruffling in TR cells, accompanied by actin depolymerization [E(-) population; 78% at 15 min after thapsigargin alone treatment].

A highly specific and well-characterized ROCK inhibitor, Y27632 (Uehata et al., 1997; Hirose et al., 1998), was used to examine the involvement of the Rho pathway. Pretreatment of cells with Y27632 did not affect LPA-induced decreases in the E(+) cell population percentages during the first several minutes after LPA exposure (Figure 3d). However, in Y27632-treated cell populations, there was no increase in the R cell population (Figure 3, c and f). Instead, a greater increase in the E(-) cell percentages was observed in Y27632-treated cells than observed in nontreated cells (Figure 3, a, b, and e). These results suggested that cells remained in the E(-) cell stage without progressing to the R cell stage. Similar results were obtained in cells pretreated with genistein, a general tyrosine kinase inhibitor (Akiyama et al., 1987) (Figure 3, a and c), consistent with the previous report (Kranenburg et al., 1999). Because genistein has little effect on PKC and other protein kinases at the concentration used (100 nM), our results indicated the involvement of tyrosine kinase in LPA-induced actin polymerization. However, how genistein-sensitive tyrosine kinase(s) interacts with the Rho pathway remains to be determined.

LPA-induced Ca²⁺ Mobilization and Rho Activation

Our pharmacological experiments have suggested two intracellular signals involved in actin rearrangement in TR cells: Ca²⁺ mobilization and Rho activation. To further confirm the data from these experiments, we directly measured both signals and PLC activity. Ca²⁺ mobilization was monitored using fura 2, a fluorescent Ca²⁺ indicator. No Ca²⁺

mobilization was observed before LPA exposure (Figure 4, a and b). However, a transient increase in Ca²⁺ concentration was detected throughout a cell body, including membrane ruffling, process shaft, and the soma after LPA exposure (Figure 4, a and b). Maximal increase was observed at 2 min after LPA stimulation, consistent with an increase of E(-) cells (Figure 2f). Such Ca²⁺ mobilization was likely to be induced by inositol trisphosphate, because LPA stimulated PLC activity in TR cells (Figure 4c). LPA-induced Rho activation was tested in pull down assay by using agarose beads-conjugated rhotekin Rho binding domain, which specifically binds active GTP-bound forms of Rho (Ren and Schwartz, 2000). Within 4 min after LPA exposure, Rho was activated, and this activation sustained for at least 1 h (Figure 4d). Together with the results using Y27632 (Figure 3), these data indicated that the Rho pathway was involved in LPA-induced process retraction by actin polymerization, as reported previously (Jalink et al., 1993; Hirose et al., 1998; Kranenburg et al., 1999), but not in actin depolymerization.

Subcellular Localization of α-Actinin and f-Actin

The state of actin polymerization is controlled with actin-binding proteins, such as actin-capping or actin cross-linking proteins. These proteins regulate polymerization of globular actin, depolymerization of f-actin, and cross-linking of f-actin in response to intracellular signaling molecules (e.g., Ca²⁺) (Bamburg and Bernstein, 1991; Bray, 1992; Janmey, 1994; Matsudaira, 1994). In view of our data suggesting the role of Ca²⁺ in LPA-induced actin depolymerization (Figures 3 and 4), the involvement of α-actinin or gelsolin, both of which are Ca²⁺-regulated actin-binding proteins, was examined. α-Actinin is an actin cross-linking protein, which has been shown to play a role in neurite outgrowth in neuronal cells and to exist within membranes ruffling of motile cells (Jockusch et al., 1983; Bamburg and Bernstein, 1991; Sobue, 1993). Binding of Ca²⁺ to a nonmuscle type of

α -actinin stimulates its dissociation from f-actin, resulting in the accumulation of free f-actin (Condeelis and Vahey, 1982). On the other hand, gelsolin is a Ca^{2+} -regulated actin-severing protein, and binding of Ca^{2+} to gelsolin leads to actin depolymerization (Bamburg and Bernstein, 1991; Janmey, 1994).

When TR cells were double labeled for α -actinin and f-actin, expression of α -actinin was observed throughout the soma, particularly within membrane ruffling where prominent f-actin labeling was observed (Figure 5, a and b). We also treated TR cells with LPA, followed by labeling for α -actinin. Within 2 min after LPA exposure, α -actinin labeling either weakened or vanished at the tips of processes with a concomitant reduction in f-actin labeling (Figure 5, c and d). Cell populations with prominent α -actinin labeling at the tips of processes decreased between 2 and 8 min, and then gradually recovered with time (Figure 5e). This temporal profile was consistent with that of E(+) cells (Figure 5e). In contrast, gelsolin distribution showed no obvious overlap with that of f-actin both in control and LPA-treated cells (Figure 5, f and g). These results indicated that LPA-induced actin depolymerization/polymerization within ruffling membranes was correlated with α -actinin accumulation, but not gelsolin, and allowed us to focus on a role of α -actinin.

The signaling pathways regulating α -actinin distribution were explored using BAPTA-AM or Y27632. Cells were pretreated with BAPTA-AM or Y27632, exposed to LPA, and then double labeled for α -actinin and f-actin. In BAPTA-AM-treated cells, α -actinin labeling was prominent and correlated with an accumulation of f-actin within membrane ruffling (Figure 6, a and b). In contrast, cells treated with Y27632 showed loss of both f-actin and α -actinin labeling at the tips of processes after LPA exposure (Figure 6, c and d), as was found in control cells (Figure 5, c and d). These data indicated that Ca^{2+} signaling, but not Rho pathways, was involved in LPA-induced loss of α -actinin and f-actin labeling within membranes ruffling.

Effects of an α -Actinin Mutant on LPA-induced Cytoskeletal Changes

α -Actinin consists of an actin-binding domain, a domain containing spectrin-like repeats, and two EF hand Ca^{2+} -binding motifs (Baron *et al.*, 1987a,b; Arimura *et al.*, 1988; Youssoufian *et al.*, 1990; Waites *et al.*, 1992) (Figure 7a). To examine the requirement of α -actinin for f-actin depolymerization, a mutant form of α -actinin that lacks two EF hand motifs [designated herein as α -actinin^(-EF)] and thereby could act as Ca^{2+} -insensitive α -actinin was constructed (Figure 7a). The expression of FLAG-tagged proteins in TR cells was confirmed by Western blot analysis by using anti-FLAG antibody (Figure 7b). Both FLAG-tagged α -actinin and α -actinin^(-EF) showed f-actin-binding activities in the absence of Ca^{2+} (Figure 7c), as expected from the reports that truncated α -actinin (without spectrin-like domains and EF motifs, or without only EF motifs) can bind f-actin (Tokue *et al.*, 1991; Hemmings *et al.*, 1992). In addition, f-actin-binding activity of α -actinin^(-EF) was expectedly Ca^{2+} -insensitive under conditions where FLAG-tagged full-length α -actinin lost the binding activity (Figure 7c). In TR cells transfected with FLAG-tagged α -actinin or α -actinin^(-EF) plasmid, FLAG immunolabeling always colocalized with f-actin, particularly within membrane ruffling (Figure 7d).

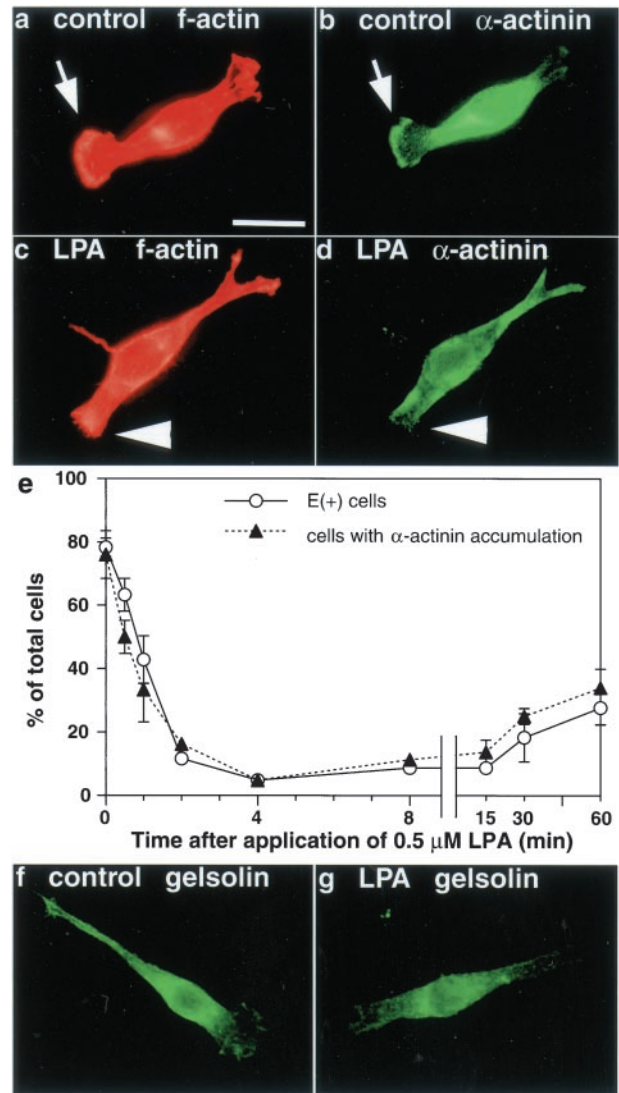


Figure 5. Colocalization of f-actin and α -actinin within membrane ruffling in TR cells. (a–d) Cells treated without (a and b) or with 0.5 μM LPA for 2 min (c and d) were labeled for f-actin (a and c) or α -actinin (b and d). Arrows indicate colocalization of f-actin and α -actinin within membrane ruffling, and arrowheads indicate LPA-induced concomitant reduction in f-actin and α -actinin labeling within membrane ruffling. (e) Time course of LPA-induced changes in E(+) cell population and those cells with prominent α -actinin labeling within membrane ruffling. Cells were treated with 0.5 μM LPA for the indicated time, fixed, and double labeled for f-actin and α -actinin. Data are the means \pm SEM ($n = 6$). (f and g) Gelsolin staining of cells treated without (f) or with 0.5 μM LPA for 2 min (g). Bar, 20 μm .

However, when these cells were double labeled for FLAG and α -actinin, no or weak labeling of α -actinin was observed within membrane ruffling of FLAG-tagged α -actinin^(-EF)-expressing cells, whereas clear labeling in FLAG-tagged α -actinin-expressing cells. Because anti- α -actinin antibody recognized α -actinin but not α -actinin^(-EF) (our unpublished data), these results indicated that the level of endogenous

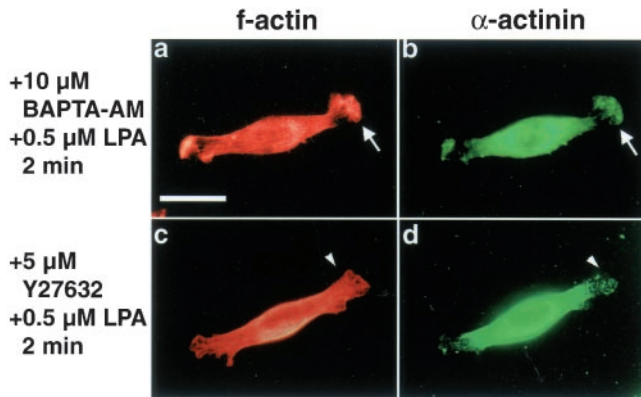


Figure 6. BAPTA-AM, but not Y27632, inhibits LPA-induced concomitant reduction in f-actin and α -actinin labeling. (a and b) f-Actin (a) and α -actinin (b) labeling of TR cells treated with 0.5 μ M LPA for 2 min in the presence of 10 μ M BAPTA-AM. Arrows indicate colocalization of f-actin and α -actinin within membrane ruffling. (c and d) f-Actin (c) and α -actinin (d) labeling of TR cells treated with 0.5 μ M LPA for 2 min in the presence of 5 μ M Y27632. Arrowheads indicate concomitant reduction in f-actin and α -actinin labeling within membrane ruffling. Bar, 20 μ m.

α -actinin decreased within membrane ruffling of α -actinin^(-EF)-expressing cells. Therefore, exogenously expressed α -actinin^(-EF) could replace endogenous α -actinin to cross-link f-actin within membrane ruffling, and perhaps fail to respond to intracellular Ca²⁺ mobilization by dissociating f-actin and thereby acts as a dominant-negative form.

TR cells were transfected with a control vector (FLAG-bacterial alkaline phosphatase; BAP), or experimental vectors [FLAG- α -actinin and FLAG- α -actinin^(-EF)], exposed to LPA for 4 min and then double labeled for f-actin and FLAG. The E(-) and E(+) cells were counted in the FLAG-positive population. In cells transfected with a control vector, LPA increased the E(-) cell population (28% increase in Figure 7e) with a concomitant decrease in the E(+) cell population (46% decrease), indicating that actin depolymerization occurred as in nontransfected cells (Figure 2f). Similar results were obtained in cells overexpressing the wild-type α -actinin (Figure 7e). In contrast, even although the expression of FLAG-tagged α -actinin^(-EF) was much lower than that of FLAG-tagged wild-type α -actinin in transfected TR cells (Figure 7b), the LPA-induced increase in the E(-) cell population was significantly attenuated by α -actinin^(-EF) overexpression (16% increase in Figure 7e). There was also a significant inhibition of the LPA-induced decrease in the E(+) cell population (29% decrease). These results indicated that overexpression of a mutant α -actinin^(-EF) inhibited LPA-induced actin depolymerization, suggesting that Ca²⁺-regulation through EF hands in α -actinin was, at least in part, responsible for LPA-induced actin depolymerization within membrane ruffling.

Effects of α -Actinin^(-EF) on LPA-induced Morphological Changes in Growth Cone of Primary Neurons

α -Actinin is known to be enriched in neuronal growth cone and suggested to be involved in its morphology (Sobue,

1993). Our finding that α -actinin also accumulated in membrane ruffling at the tips of growing processes of TR cells led us to examine a role of LPA-induced actin depolymerization in growth cone morphology of primary neurons. We used primary cultures consisting of young cortical neurons in which neurite outgrowth was underway and *lpa*₂ was expressed (Fukushima *et al.*, 2002). These neurons expressed endogenous α -actinin at their growth cone and cell body, colocalized with f-actin (Figure 8, a and b). This overlap was similar to that observed in TR cells, although the fluorescence intensities of these components were not as high as those in TR cells. In control, 38.9% of total neurons possessed intact growth cones, defined as f-actin-enriched, flat and wider structures than neurites. When LPA was exposed to these neurons for 4 min, the population with growth cones was decreased to 16.7%, indicating that LPA induced growth cone collapse. However, no marked process retraction and cell rounding were not observed, probably because these cellular responses were reduced with the progress of morphological maturation of neurons (Fukushima *et al.*, 2002). Similar growth cone collapse was observed in neurons transfected with a control FLAG-BAP vector (Figure 8, c-f, the population with growth cone in transfected neurons; 46.2% in control vs. 23.8% in LPA treatment). In contrast, LPA treatment failed to induce marked changes in growth cone morphology of α -actinin^(-EF)-expressing neurons (Figure 8, g-j, the population with growth cone in transfected neurons; 46.5% in control vs. 43.8% in LPA treatment). These results indicated that LPA-induced actin depolymerization through α -actinin was involved in regulation of growth cone morphology of primary neurons.

Heterologous Expression of LPA Receptors *lpa*₁ or *lpa*₂

Two LPA receptors expressed in TR cells, LPA₁ and LPA₂, have similar signaling properties, including PLC activation and Rho stimulation (Fukushima *et al.*, 1998, 2001; Ishii *et al.*, 2000; Kimura *et al.*, 2001). On the other hand, the LPA molecule itself can directly interact with actin-binding proteins (Meerschaert *et al.*, 1998), and these interactions might be involved in the LPA-induced actin depolymerization. To determine whether LPA receptors or nonreceptor mechanisms are involved in actin depolymerization, either *lpa*₁ or *lpa*₂ was heterologously expressed using retrovirus expression systems in a B103 rat neuroblastoma cell line. This cell line expresses none of the three known LPA receptors and shows no cytoskeletal responses to LPA, but responds to LPA with process retraction when either *lpa*₁ or *lpa*₂ is introduced (Fukushima *et al.*, 1998; Ishii *et al.*, 2000; Kimura *et al.*, 2001).

Cells were infected with *lpa*₁-expressing retroviruses that coexpress EGFP, and then double labeled for EGFP and either f-actin or α -actinin. Infected (EGFP-positive) cells showed marked f-actin labeling as well as α -actinin labeling within membrane ruffling as was observed in TR cells (Figure 9, a, b, e, and f). LPA treatment for 2 min resulted in reduced labeling within the tips of processes (Figure 9, c, d, g, h, and i). Such changes in f-actin and α -actinin labeling were also observed in *lpa*₂-expressing cells (Figure 9i). In the absence of exogenous *lpa*₁ or *lpa*₂ expression, actin depolymerization was not observed (Figure 9i). Combined with our previous data (Fukushima

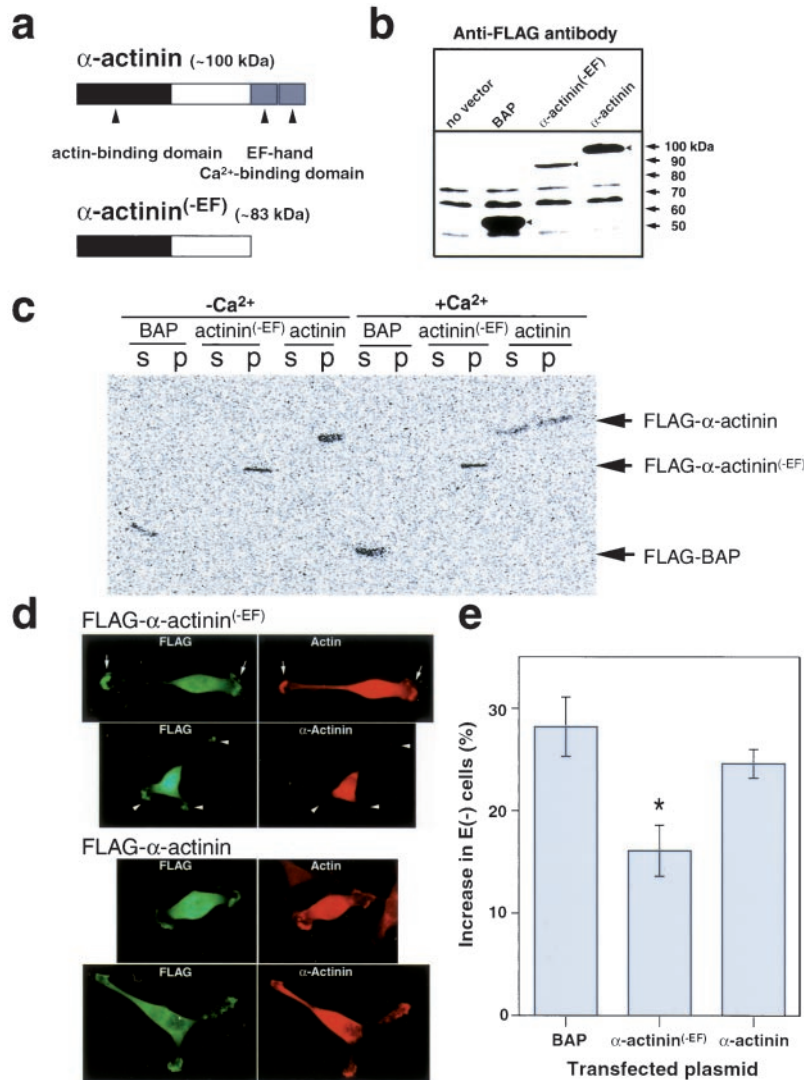


Figure 7. Overexpression of Ca²⁺-insensitive mutant α -actinin inhibits LPA-induced actin depolymerization in membrane ruffling. (a) Schematic illustration of protein structures of α -actinin and α -actinin^(-EF), a mutant form lacking two EF hands. (b) Western blot analyses of transfected TR cells to detect overexpressed FLAG-tagged proteins. Non-transfected or transfected cells with a control vector (FLAG-BAP), α -actinin^(-EF), or α -actinin expression vector were analyzed using anti-FLAG antibody. Arrowheads indicate overexpressed FLAG-tagged proteins. (c) f-Actin binding of FLAG-tagged α -actinin and α -actinin^(-EF). Tagged proteins were immunoprecipitated from TR cell extracts and used for f-actin-binding assay in the absence or presence of Ca²⁺. Unbound (s) and bound (p) fractions were subjected to Western blot analysis to detect FLAG. (d) FLAG, f-actin, and α -actinin labeling of transfected TR cells. Transfected cells were double labeled for FLAG and f-actin, or FLAG and α -actinin. Arrows indicate typical membrane ruffling that contains α -actinin^(-EF) and f-actin. Arrowheads indicate typical membrane ruffling that contains α -actinin^(-EF) and low levels of endogenous α -actinin. (e) Effects of α -actinin^(-EF) overexpression on LPA-induced increase in E(-) cell population. TR cells were transfected and treated without or with 0.5 μ M LPA. Cells were fixed at 4 min and double labeled for f-actin and FLAG, and E(-) cells were counted. Data are the means \pm SEM (n = 4). *p < 0.05 α -actinin^(-EF) vs. BAP.

et al., 1998; Ishii *et al.*, 2000), both LPA₁ and LPA₂ appeared capable of explaining LPA-induced actin depolymerization associated with membrane ruffling as well as actin polymerization in neurite shafts.

DISCUSSION

We have shown herein that LPA induces two distinct forms of actin rearrangement within single neuroblasts: depolymerization associated with loss of membrane ruffling, and polymerization associated with process retraction. A single type of LPA receptor regulates each actin rearrangement by activating distinct cellular signaling pathways: depolymerization via Ca²⁺- α -actinin and actin polymerization via Rho. These results suggest a novel role for receptor-mediated LPA signaling in regulation of the actin cytoskeleton in neuronal cells.

LPA Induces Both Actin Depolymerization and Polymerization within a Single Cell

Actin microfilaments are primarily regulated through their interactions with actin-binding proteins and/or intracellular signaling messengers produced by extracellular stimuli such as growth factors and extracellular matrix (ECM) (Bamburg and Bernstein, 1991; Bray, 1992; Janmey, 1994; Matsudaira, 1994). Depending on the types of interactions, cells can undergo either polymerization or depolymerization to change their morphologies (e.g., leading edge of migrating cells).

LPA has been shown to be a potent inducer of actin polymerization (Moolenaar, 1995, 1997). LPA-induced actin polymerization results in process retraction and cell rounding in neuronal cells such as N1E-115, or stress fiber formation in fibroblast cells (Ridley and Hall, 1992; Jalink *et al.*, 1993). These cellular responses are mediated by actomyosin interactions through activation of the Rho pathway, produc-

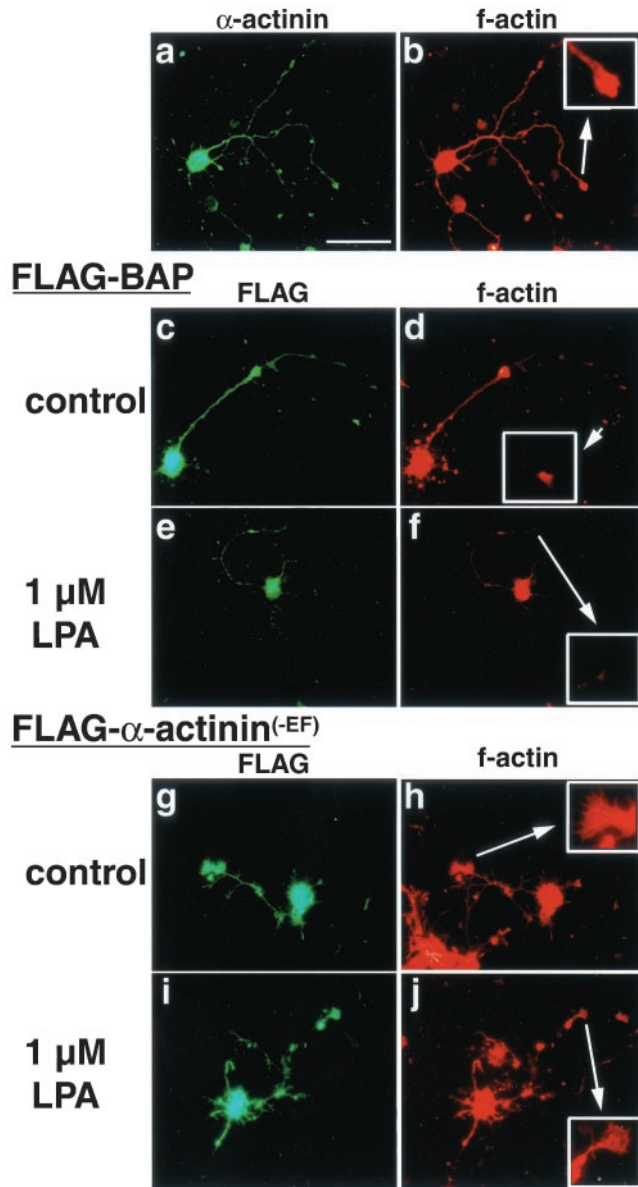


Figure 8. Overexpression of α -actinin^(-EF) inhibits LPA-induced growth cone collapse. (a and b) α -Actinin (a) and f-actin (b) labeling of primary cortical neurons cultured for 5 d. (c–f) Typical FLAG (c and e) and f-actin (d and f) labeling of cortical neurons transfected with a FLAG-BAP plasmid. Neurons were treated without (c and d) or with 0.5 μ M LPA for 4 min (e and f), and double labeled for FLAG and f-actin. (g–j) Typical FLAG (g and i) and f-actin (h and j) labeling of cortical neurons transfected with a FLAG- α -actinin^(-EF) plasmid. Neurons were treated without (g and h) or with 0.5 μ M LPA for 4 min (i and j), and double labeled for FLAG and f-actin. Insets are 3 \times magnifications of growth cones. Growth cones in b, d, h, and j are defined to be intact by f-actin–enriched, flat, and wider structures than neurites, whereas growth cone in f is collapsed. Bar, 20 μ m.

ing contractile forces that induce cell shape changes (Jalink *et al.*, 1994; Tigyi *et al.*, 1996; Kozma *et al.*, 1997; Hirose *et al.*, 1998; Kranenburg *et al.*, 1999; Fukushima *et al.*, 2000; Weiner

et al., 2001). Herein, we have also shown that Rho is activated by LPA in TR cells and LPA-induced process retraction is blocked by a ROCK inhibitor or CD, which indicates the possible involvement of Rho and actomyosin for process retraction in TR cells (Figure 10).

In addition to actin-polymerizing effects, LPA induced more rapid, transient actin depolymerization within the same cell. It is possible that depolymerized actin could be the source for subsequent actin polymerization during process retraction. However, this is unlikely because BAPTA-AM did not block LPA-induced process retraction, whereas Y27632 failed to inhibit LPA-induced loss of f-actin within membrane ruffling. Therefore, LPA appears to activate two independent signaling pathways, with opposing effects on the actin rearrangement, and apparently using distinct pools of actin. Our results also suggest that actin rearrangement induced by LPA may be compartmentalized; actin depolymerization associated with membrane ruffling occurs at the tips of processes, whereas actin polymerization occurs in the shaft of processes (Figure 10).

LPA-induced actin depolymerization has not been documented previously, perhaps because of the use of different cell types or different techniques that focused on longer time periods after LPA exposure. For example, fibroblasts have little cytoplasmic f-actin in resting conditions (i.e., G₀ phase of cell cycle) (Ridley and Hall, 1992), and actin depolymerization might not be detectable after stimulation of the cells. In neuronal cells, actin rearrangement has been examined by fluorometric methods that monitor changes in f-actin in the entire cell body (Jalink *et al.*, 1993), and these methods might not detect local fine changes in f-actin levels.

LPA-induced Actin Depolymerization Involves Ca²⁺- α -Actinin but Not Rho

Several lines of evidence in the present study support an idea that LPA-induced actin depolymerization is mediated by Ca²⁺- α -actinin interactions: 1) α -actinin was colocalized with enriched f-actin within membrane ruffling, and both dissipated after LPA exposure; 2) pretreatment with a Ca²⁺ chelator, BAPTA-AM, inhibited LPA-induced loss of membrane ruffling; 3) intracellular Ca²⁺ mobilization was induced in membrane ruffling after LPA stimulation; and 4) overexpression of Ca²⁺-insensitive α -actinin^(-EF), which binds f-actin and replaces endogenous α -actinin, attenuated LPA-induced actin depolymerization. LPA-induced increases in Ca²⁺ concentration within membrane ruffling perhaps inhibit the actin cross-linking activity of α -actinin through its EF hands, which in turn leads to the dissociation of α -actinin from f-actin (Bamburg and Bernstein, 1991; Janmey, 1994) (Figure 10). However, actin depolymerization observed as the disappearance of f-actin labeling should normally require actin-depolymerizing or actin-severing activity, which has not been documented for α -actinin. This suggests involvement of another mechanism for actin depolymerization after dissociation of actin filaments resulting from the inhibition of α -actinin activity.

α -Actinin is also known to link actin filaments to receptors for ECM molecules (Pavalko *et al.*, 1991). It has been shown that complexes containing α -actinin, ECM, and ECM receptors are involved in the formation of membrane ruffling (Jockusch *et al.*, 1983; O'Connor *et al.*, 2000).

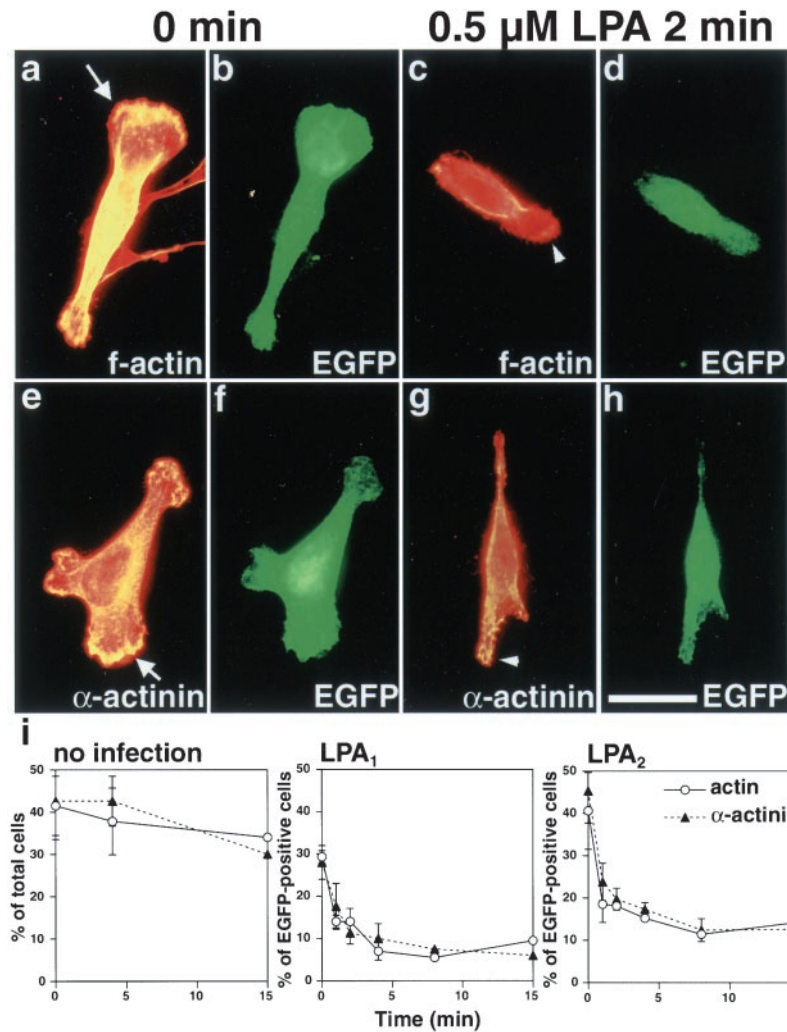


Figure 9. Heterologous expression of LPA₁ or LPA₂ is sufficient for LPA-induced actin depolymerization in B103 cells. (a–d) f-Actin (a and c) and EGFP (b and d) labeling of B103 cells infected with retroviruses expressing *lpa₁*. Cells were treated without (a and b) or with 0.5 μM LPA for 2 min (c and d), and double labeled for f-actin and EGFP. An arrow (a) indicates a process with f-actin-enriched membrane ruffling. An arrowhead (c) indicates a process without f-actin-enriched structures. (e–h) α-Actinin (e and g) and EGFP (f and h) labeling of B103 cells infected with retroviruses expressing *lpa₁*. Cells were treated without (e and f) or with 0.5 μM LPA for 2 min (g and h) and double labeled for α-actinin and EGFP. An arrow (e) indicates a process with α-actinin-enriched membrane ruffling. An arrowhead (g) indicates a process without α-actinin-enriched structures. (i) Time course of LPA-induced reduction in B103 cell populations with enriched f-actin or α-actinin. B103 cells infected with retroviruses expressing *lpa₁* or *lpa₂* were treated with 0.5 μM LPA. Cells were fixed at the indicated time and double labeled for f-actin and EGFP or α-actinin and EGFP. E(+) cells and cells with prominent α-actinin labeling within membrane ruffling were counted in naive cells (left) or cells infected to express *lpa₁* (middle) or *lpa₂* (right). Data are the means ± SEM (n = 4–6). Bar, 20 μm.

We detected the distribution of β1-integrin, one of the ECM receptors, in membrane ruffling of TR cells by immunocytochemical labeling (our unpublished data). LPA-induced loss of membrane ruffling may involve dissociation of actin filaments from those complexes as well as between filaments.

Our data show a role for α-actinin in actin rearrangement that is different from previous results observed in several cell types. In fibroblasts, α-actinin is recruited along f-actin stress fibers and focal adhesions in response to serum or LPA stimulation (Barry and Critchley, 1994). These cells are likely to use α-actinin in actin rearrangement primarily directed toward polymerization in a Rho-dependent manner, which is different from our data on neuronal cells presented herein. Whether α-actinin is also involved in actin polymerization in TR cells remains to be determined. However, this seems unlikely because overexpression of α-actinin or α-actinin^(-EF) did not alter LPA-induced process retraction (our unpublished data). Thus, in LPA-stimulated TR cells, α-actinin appears to play a role in actin depolymerization but not in actin polymerization.

Both LPA₁ and LPA₂ Could Mediate LPA-induced Actin Depolymerization and Polymerization

Both LPA₁ and LPA₂ can stimulate PLC through PTX-insensitive G proteins (e.g., G_q) in neuronal cells (Ishii *et al.*, 2000; Kimura *et al.*, 2001), producing inositol trisphosphate that induces Ca²⁺ release from intracellular Ca²⁺ stores (Berridge, 1993). This Ca²⁺ mobilization by activation of the G_q-PLC pathway has been also confirmed in the present study (Figure 4) and is probably involved in the inhibition of α-actinin activity (Bamburg and Bernstein, 1991; Janmey, 1994). Both LPA receptors can also activate the Rho pathway that is linked to myosin stimulation, which leads to actin polymerization (Amano *et al.*, 1998; Fukushima *et al.*, 1998; Ishii *et al.*, 2000). Thus, a single LPA receptor is likely to use two independent signaling pathways for actin regulation. This idea is supported by the data from our heterologous experiments using B103 cells, which demonstrated that expression of either LPA receptor was enough for dual regulation of actin rearrangement.

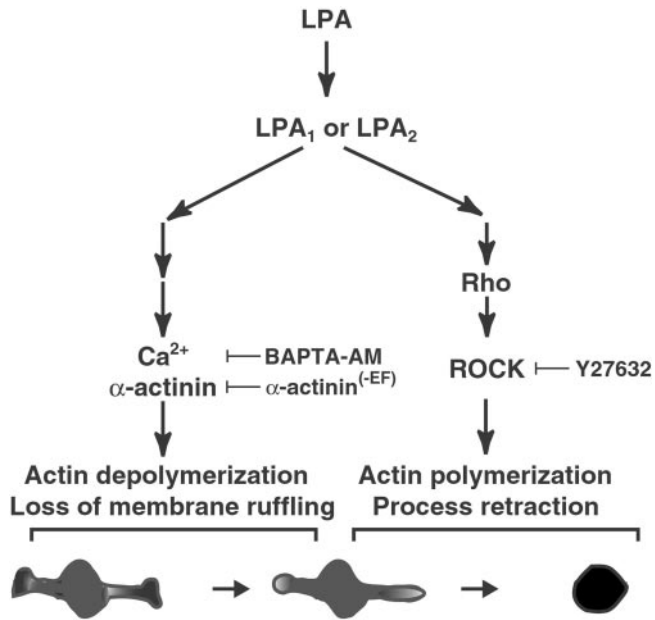


Figure 10. Proposed model for dual regulation of actin rearrangement by diverging intracellular signals from a single LPA receptor. Either LPA_1 or LPA_2 receptors can mediate two distinct types of actin rearrangement in TR cells: actin depolymerization and polymerization. In membrane ruffling, actin is depolymerized through Ca^{2+} - α -actinin interactions, whereas in neurite shafts, actin is polymerized via the Rho pathway. These distinct pathways may coordinate to regulate morphology of neuronal cells.

Possible Roles for LPA-induced Actin Rearrangements in Neuronal Cell Morphology

TR cells show many features of cortical neuroblasts (e.g., expression of neuroblast markers, such as brain factor-1, lpa_1 , and nestin [an intermediate filament protein]), but also express early neuronal markers, such as neurofilament proteins (Chun and Jaenisch, 1996). Therefore, these cells provide a good, homogenous model system to study intracellular events that occur in primary neuroblasts or migrating or differentiating neurons. Cortical neuroblasts express lpa_1 (Hecht *et al.*, 1996) and extend radially oriented processes and undergo a "to-and-fro movement," called interkinetic nuclear migration, in which process retraction and extension are repeated with a radial nuclear movement (Seymour and Berry, 1975). Our previous study has shown that LPA signaling affects cortical neuroblast morphology through actin polymerization (Fukushima *et al.*, 2000). However, how actin depolymerization is involved in the neuroblast morphology remains uncertain. α -Actinin may form a complex with actin filaments and focal adhesion proteins, which functions as scaffolds for signal transduction and/or the attachment of processes (Barry and Critchley, 1994), although its precise localization in neuroblasts remains to be determined. Actin depolymerization through Ca^{2+} - α -actinin interactions may produce loss of these scaffolds and/or the detachment of processes, an essential step of interkinetic nuclear migration (Fukushima *et al.*, 2000).

Migrating or differentiating neurons express lpa_2 (Fukushima *et al.*, 2002) and extend leading processes during

migration of axons and dendrites at their final destination, respectively. Ca^{2+} is an important factor for the regulation of growth cone morphology in these processes (Letourneau, 1996), and both α -actinin and f-actin are concentrated in the filopodia of growth cone (Sobue and Kanda, 1989). Our data from the experiments using primary neurons suggest the involvement of Ca^{2+} - α -actinin interactions in LPA-induced changes in growth cone morphology, which would implicate LPA as a guidance molecule for migrating or differentiating neurons. Clearly, further investigation should be necessary for clarifying the biologically relevant roles for LPA-induced dual actin rearrangement in the nervous system.

ACKNOWLEDGMENTS

We thank Carol Akita and Marisa Fontanoz for technical assistance, Drs. Joshua A. Weiner and Dhruv Kaushal for reading the manuscript, Dr. Takaharu Yamamoto for f-actin binding assay, and Casey Cox for copyediting the manuscript. This work was supported by the National Institute of Mental Health and an unrestricted gift from Merck Research Laboratories (to J.C.) and by the Ministry of Education, Science, Sports and Culture of Japan (to N.F. and Y.H.).

REFERENCES

- Akiyama, T., Ishida, J., Nakagawa, S., Ogawara, H., Watanabe, S., Itoh, N., Shibuya, M., and Fukami, Y. (1987). Genistein, a specific inhibitor of tyrosine-specific protein kinases. *J. Biol. Chem.* 262, 5592-5595.
- Amano, M., Chihara, K., Kimura, K., Fukata, Y., Nakamura, N., Matsuura, Y., and Kaibuchi, K. (1997). Formation of actin stress fibers and focal adhesions enhanced by Rho-kinase. *Science* 275, 1308-1311.
- Amano, M., Chihara, K., Nakamura, N., Fukata, Y., Yano, T., Shibata, M., Ikebe, M., and Kaibuchi, K. (1998). Myosin II activation promotes neurite retraction during the action of Rho and Rho-kinase. *Genes Cells* 3, 177-188.
- An, S., Bleu, T., Hallmark, O.G., and Goetzl, E.J. (1998). Characterization of a novel subtype of human G protein-coupled receptor for lysophosphatidic acid. *J. Biol. Chem.* 273, 7906-7910.
- Arimura, C., Suzuki, T., Yanagisawa, M., Imamura, M., Hamada, Y., and Masaki, T. (1988). Primary structure of chicken skeletal muscle and fibroblast α -actinins deduced from cDNA sequences. *Eur. J. Biochem.* 177, 649-655.
- Bamburg, J.R., and Bernstein, B.W. (1991). Actin and actin-binding proteins in neurons. In: *The Neuronal Cytoskeleton*, ed. R.D. Burgoyne, New York: Wiley-Liss, 121-160.
- Bandoh, K., Aoki, J., Hosono, H., Kobayashi, S., Kobayashi, T., Murakami-Murofushi, K., Tsujimoto, M., Arai, H., and Inoue, K. (1999). Molecular cloning and characterization of a novel human G-protein-coupled receptor, EDG7, for lysophosphatidic acid. *J. Biol. Chem.* 274, 27776-27785.
- Baron, M.D., Davison, M.D., Jones, P., and Critchley, D.R. (1987a). The sequence of chick α -actinin reveals homologies to spectrin and calmodulin. *J. Biol. Chem.* 262, 17623-17629.
- Baron, M.D., Davison, M.D., Jones, P., Patel, B., and Critchley, D.R. (1987b). Isolation and characterization of a cDNA encoding a chick α -actinin. *J. Biol. Chem.* 262, 2558-2561.
- Barry, S.T., and Critchley, D.R. (1994). The RhoA-dependent assembly of focal adhesions in Swiss 3T3 cells is associated with increased tyrosine phosphorylation and the recruitment of both pp125FAK and protein kinase C- δ to focal adhesions. *J. Cell Sci.* 107, 2033-2045.

- Berridge, M.J. (1993). Inositol trisphosphate and calcium signaling. *Nature* 361, 315–325.
- Bray, D. (1992). *Cell Movements*, New York: Garland Pub.
- Chun, J. (1999). Lysophospholipid receptors: implications for neural signaling. *Crit. Rev. Neurobiol.* 13, 151–168.
- Chun, J., Contos, J.J.A., and Munroe, D. (1999). A growing family of receptor genes for lysophosphatidic acid (LPA) and other lysophospholipids (LPs). *Cell Biochem. Biophys.* 30, 213–242.
- Chun, J., and Jaenisch, R. (1996). Clonal cell lines produced by infection of neocortical neuroblasts using multiple oncogenes transduced by retroviruses. *Mol. Cell. Neurosci.* 7, 304–321.
- Condeelis, J., and Vahey, M. (1982). A calcium- and pH-regulated protein from *Dictyostelium discoideum* that cross-links actin filaments. *J. Cell Biol.* 94, 466–471.
- Contos, J.J.A., and Chun, J. (1998). Complete cDNA sequence, genomic structure, and chromosomal localization of the LPA receptor gene, *lp_{A1}/vzg-1/Gpcr26*. *Genomics* 51, 364–378.
- Contos, J.J.A., Ishii, I., and Chun, J. (2000). Lysophosphatidic acid receptors. *Mol. Pharmacol.* 58, 1188–1196.
- Fukushima, N., Ishii, I., Contos, J.A., Weiner, J.A., and Chun, J. (2001). Lysophospholipid receptors. *Annu. Rev. Pharmacol. Toxicol.* 41, 507–534.
- Fukushima, N., Kimura, Y., and Chun, J. (1998). A single receptor encoded by *vzg-1/lp_{A1}/edg-2* couples to G proteins and mediates multiple cellular responses to lysophosphatidic acid. *Proc. Natl. Acad. Sci. USA* 95, 6151–6156.
- Fukushima, N., Weiner, J.A., and Chun, J. (2000). Lysophosphatidic acid (LPA) is a novel extracellular regulator of cortical neuroblast morphology. *Dev. Biol.* 228, 6–18.
- Fukushima, N., Weiner, J.A., Kaushal, D., Contos, J.J.A., Rehen, S.K., Kingsbury, M.A., Kim, K.-Y., and Chun, J. (2002). Lysophosphatidic acid influences the morphology, and motility of young, postmitotic cortical neurons. *Mol. Cell. Neurosci.* 20, 271–282.
- Gohla, A., Harhammer, R., and Schultz, G. (1998). The G-protein G₁₃ but not G₁₂ mediates signaling from lysophosphatidic acid receptor via epidermal growth factor receptor to Rho. *J. Biol. Chem.* 273, 4653–4659.
- Habara, Y., and Kanno, T. (1991). Dose-dependency in spatial dynamics of [Ca²⁺]_i in pancreatic acinar cells. *Cell Calcium* 12, 533–542.
- Hecht, J.H., Weiner, J.A., Post, S.R., and Chun, J. (1996). *Ventricular zone gene-1 (vzg-1)* encodes a lysophosphatidic acid receptor expressed in neurogenic regions of the developing cerebral cortex. *J. Cell Biol.* 135, 1071–1083.
- Hemmings, L., Kuhlman, P.A., and Critchley, D.R. (1992). Analysis of the actin-binding domain of α -actinin by mutagenesis and demonstration that dystrophin contains a functionally homologous domain. *J. Cell Biol.* 116, 1369–1380.
- Hirose, M., Ishizaki, T., Watanabe, N., Uehata, M., Kranenburg, O., Moolenaar, W.H., Matsumura, F., Maekawa, M., Bito, H., and Narumiya, S. (1998). Molecular dissection of the Rho-associated protein kinase p160ROCK-regulated neurite remodeling in neuroblastoma N1E-115 cells. *J. Cell Biol.* 141, 1625–1636.
- Ishii, I., Contos, J.J., Fukushima, N., and Chun, J. (2000). Functional comparisons of the lysophosphatidic acid receptors, LP_{A1}/VZG-1/EDG-2, LP_{A2}/EDG-4, and LP_{A3}/EDG-7 in neuronal cell lines using a retrovirus expression system. *Mol. Pharmacol.* 58, 895–902.
- Jalink, K., Eichholtz, T., Postma, F.R., van Corven, E.J., and Moolenaar, W.H. (1993). Lysophosphatidic acid induces neuronal shape changes via a novel, receptor-mediated signaling pathway: similarity to thrombin action. *Cell Growth Differ.* 4, 247–255.
- Jalink, K., van Corven, E.J., Hengeveld, T., Morii, N., Narumiya, S., and Moolenaar, W.H. (1994). Inhibition of lysophosphatidate- and thrombin-induced neurite retraction and neuronal cell rounding by ADP ribosylation of the small GTP-binding protein Rho. *J. Cell Biol.* 126, 801–810.
- Janmey, P.A. (1994). Phosphoinositides and calcium as regulators of cellular actin assembly and disassembly. *Annu. Rev. Physiol.* 56, 169–191.
- Jockusch, B.M., Haemmerli, G., and In Albon, A. (1983). Cytoskeletal organization in locomoting cells of the V2 rabbit carcinoma. *Exp. Cell Res.* 144, 251–263.
- Katada, T., Oinuma, M., and Ui, M. (1986). Two guanine nucleotide-binding proteins in rat brain serving as the specific substrate of islet-activating protein, pertussis toxin. Interaction of the α -subunits with $\beta\gamma$ subunits in development of their biological activities. *J. Biol. Chem.* 261, 8182–8191.
- Keenan, C., and Kelleher, D. (1998). Protein kinase C and the cytoskeleton. *Cell. Signal.* 10, 225–232.
- Kimura, Y., Schmitt, A., Fukushima, N., Ishii, I., Kimura, H., Nebreda, A.R., and Chun, J. (2001). Two novel *Xenopus* homologs of mammalian LP_{A1}/EDG-2 function as lysophosphatidic acid receptors in *Xenopus* oocytes and mammalian cells. *J. Biol. Chem.* 276, 15208–15215.
- Kozma, R., Sarner, S., Ahmed, S., and Lim, L. (1997). Rho family GTPases and neuronal growth cone remodeling: relationship between increased complexity induced by Cdc42Hs, Rac1, and acetylcholine and collapse induced by RhoA and lysophosphatidic acid. *Mol. Cell. Biol.* 17, 1201–1211.
- Kranenburg, O., Poland, M., van Horck, F.P., Drechsel, D., Hall, A., and Moolenaar, W.H. (1999). Activation of RhoA by lysophosphatidic acid and G α 12/13 subunits in neuronal cells: induction of neurite retraction. *Mol. Cell Biol.* 19, 1851–1857.
- Laemmli, U.K. (1970). Cleavage of structural proteins during the assembly of the head of bacteriophage T4. *Nature* 227, 680–685.
- Letourneau, P.C. (1996). The cytoskeleton in nerve growth cone motility and axonal pathfinding. *Perspect. Dev. Neurobiol.* 4, 111–123.
- Manning, T.J.J., and Sontheimer, H. (1997). Bovine serum albumin and lysophosphatidic acid stimulate calcium mobilization and reversal of cAMP-induced stellation in rat spinal cord astrocytes. *Glia* 20, 163–172.
- Matsudaira, P. (1994). Actin crosslinking proteins at the leading edge. *Semin. Cell Biol.* 5, 165–174.
- Meerschaert, K., De Corte, V., De Ville, Y., Vandekerckhove, J., and Gettemans, J. (1998). Gelsolin and functionally similar actin-binding proteins are regulated by lysophosphatidic acid. *EMBO J.* 17, 5923–5932.
- Moolenaar, W.H. (1995). Lysophosphatidic acid signaling. *Curr. Opin. Cell Biol.* 7, 203–210.
- Moolenaar, W.H. (1999). Bioactive lysophospholipids and their G protein-coupled receptors. *Exp. Cell Res.* 253, 230–238.
- Moolenaar, W.H., Kranenburg, O., Postma, F.R., and Zondag, G.C. (1997). Lysophosphatidic acid: G-protein signaling and cellular responses. *Curr. Opin. Cell Biol.* 9, 168–173.
- O'Connor, K.L., Nguyen, B.-K., and Mercurio, A.M. (2000). RhoA function in lamellae formation, and migration is regulated by the α 6 β 4 integrin, and cAMP metabolism. *J. Cell Biol.* 148, 253–258.
- Pavalko, F.M., Otey, C.A., Simon, K.O., and Burridge, K. (1991). α -Actinin: a direct link between actin and integrins. *Biochem. Soc. Trans.* 19, 1065–1069.

- Ren, X., and Schwartz, M. (2000). Determination of GTP loading on Rho. *Methods Enzymol.* 325, 264–272.
- Ridley, A.J., and Hall, A. (1992). The small GTP-binding protein rho regulates the assembly of focal adhesions and actin stress fibers in response to growth factors. *Cell* 70, 389–399.
- Seymour, R.M., and Berry, M. (1975). Scanning and transmission electron microscope studies of interkinetic nuclear migration in the cerebral vesicles of the rat. *J. Comp. Neurol.* 160, 105–125.
- Shahrestanifar, M., Fan, X., and Manning, D.R. (1999). Lysophosphatidic acid activates NF- κ B in fibroblasts. A requirement for multiple inputs. *J. Biol. Chem.* 274, 3828–3833.
- Sobue, K. (1993). Actin-based cytoskeleton in growth cone activity. *Neurosci. Res.* 18, 91–102.
- Sobue, K., and Kanda, K. (1989). α -Actinins, caldesmon (brain spectrin or fodrin), and actin participate in adhesion and movement of growth cones. *Neuron* 3, 311–319.
- Thastrup, O., Cullen, P., Drobak, B., Hanley, M., and Dawson, A. (1990). Thapsigargin, a tumor promoter, discharges intracellular Ca^{2+} stores by specific inhibition of the endoplasmic reticulum Ca^{2+} -ATPase. *Proc. Natl. Acad. Sci. USA* 87, 2466–2470.
- Tigyi, G., Fischer, D.J., Sebok, A., Marshall, F., Dyer, D.L., and Miledi, R. (1996). Lysophosphatidic acid-induced neurite retraction in PC12 cells: neurite-protective effects of cyclic AMP signaling. *J. Neurochem.* 66, 549–558.
- Tokuue, Y., Goto, S., Imamura, M., Obinata, T., Masaki, T., and Endo, T. (1991). Transfection of chicken skeletal muscle α -actinin cDNA into nonmuscle and myogenic cells: dimerization is not essential for α -actinin to bind to microfilaments. *Exp. Cell Res.* 197, 158–167.
- Toullec, D., *et al.* (1991). The bisindolylmaleimide GF 109203X is a potent and selective inhibitor of protein kinase C. *J. Biol. Chem.* 266, 15771–15781.
- Uehata, M., *et al.* (1997). Calcium sensitization of smooth muscle mediated by a Rho-associated protein kinase in hypertension. *Nature* 389, 990–994.
- Waites, G., Graham, I., Jackson, P., Millake, D., Patel, B., Blanchard, A., Weller, P., Eperon, I., and Critchley, D. (1992). Mutually exclusive splicing of calcium-binding domain exons in chick α -actinin. *J. Biol. Chem.* 267, 6263–6271.
- Weiner, J.A., and Chun, J. (1999). Schwann cell survival mediated by the signaling phospholipid lysophosphatidic acid. *Proc. Natl. Acad. Sci. USA* 96, 5233–5238.
- Weiner, J.A., Fukushima, N., Contos, J.J.A., Scherer, S.S., and Chun, J. (2001). Regulation of Schwann cell morphology and adhesion by receptor-mediated lysophosphatidic acid signaling. *J. Neurosci.* 21, 7069–7078.
- Youssoufian, H., McAfee, M., and Kwiatkowski, D.J. (1990). Cloning and chromosomal localization of the human cytoskeletal α -actinin gene reveals linkage to the beta-spectrin gene. *Am. J. Hum. Genet.* 47, 62–71.